Kinetic Modelling of Transport Inhibition by Substrates in ABC Importers

de Boer, Marijn; Cordes, Thorben; Poolman, Bert

Published in:
Journal of Molecular Biology

DOI:
10.1016/j.jmb.2020.08.008

Publication date:
2020

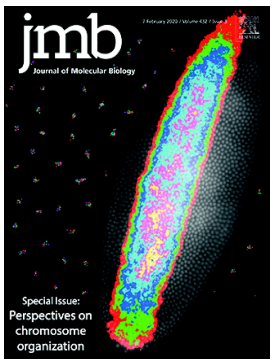

Kinetic Modelling of Transport Inhibition by Substrates in ABC Importers

Marijn de Boer, Thorben Cordes, Bert Poolman

PII: S0022-2836(20)30492-7

DOI: https://doi.org/10.1016/j.jmb.2020.08.008

Reference: YJMBI 66623

To appear in: *Journal of Molecular Biology*

Received date: 24 June 2020

Revised date: 5 August 2020

Accepted date: 9 August 2020

Please cite this article as: M. de Boer, T. Cordes and B. Poolman, Kinetic Modelling of Transport Inhibition by Substrates in ABC Importers, *Journal of Molecular Biology* (2020), https://doi.org/10.1016/j.jmb.2020.08.008

Kinetic modelling of transport inhibition by substrates in ABC importers

Marijn de Boer[1,2], Thorben Cordes[1,3] and Bert Poolman[2]

[1]Molecular Microscopy Research Group, Zernike Institute for Advanced Material, University of Groningen, Groningen, The Netherlands.
[2]Department of Biochemistry, Groningen Biomolecular Sciences and Biotechnology Institute, University of Groningen, Groningen, The Netherlands.
[3]Physical and Synthetic Biology, Faculty of Biology, Ludwig-Maximilians-Universität München, Großhadernerstr. 2-4, 82152 Planegg-Martinsried, Germany

Correspondence to marijndeboer4@gmail.com or b.poolman@rug.nl

Prokaryotic ATP-binding cassette (ABC) importers require a substrate-binding protein (SBP) for the capture and delivery of the cognate substrate to the transmembrane domain (TMD) of the transporter. Various biochemical compounds have been identified that bind to the SBP but are not transported. The mechanistic basis for the 'non-cognate' substrates not being transported differs. Some non-cognate substrates fail to trigger the appropriate conformational change in the SBP, resulting in loss of affinity for the TMD or the inability to allosterically activate transport. In another mechanism, the SBP cannot release the bound non-cognate substrate. Here, we used rate equations to derive the steady-state transport rate of cognate substrates of an ABC importer and investigated how non-cognate substrates influence this rate. We found that under limiting non-cognate substrate concentrations, the transport rate remains unaltered for each of the mechanisms. In contrast, at saturating substrate and SBP concentrations, the effect of the non-cognate substrate depends heavily on the respective mechanism. For instance, the transport rate becomes zero when the non-cognate substrate cannot be released by the SBP. Yet it remains unaffected when substrate release is possible but the SBP cannot dock onto the TMDs. Our work shows how the different mechanisms of substrate inhibition impact the transport kinetics, which is relevant for understanding and manipulating solute fluxes and hence the propagation of cells in nutritionally complex milieus.

Graphical abstract

Introduction

ATP-binding cassette (ABC) transporters form a large family of membrane transport proteins[1-3] with a common domain architecture. The translocator unit is composed of two transmembrane domains (TMDs), which form the translocation pathway for the substrate, and two cytoplasmic nucleotide-binding domains (NBDs), which bind and hydrolyse ATP. ABC transporters use the energy of ATP hydrolysis to transport various compounds, such as sugars, amino acids, vitamins, compatible solutes, metal ions, antibiotics, lipids, polypeptides, and many others[1]. Some ABC transporters are specific for a single compound[4], whereas others have broad substrate specificity and are able to transport multiple compounds[5,6]. The proposed transport mechanism of ABC transporters is based on the alternating access model[7,8], in which the translocator switches between inward- and outward-facing conformations to expose a substrate binding cavity on alternate sides of the membrane.

ABC importers are typical of prokaryotic organisms but recently a number of proteins with the 'exporter fold' have been discovered that mediate cellular uptake, both in prokaryotic and eukaryotic cells[9,10]. Both Type I and II ABC importers require a soluble extracellular or periplasmic substrate-binding protein (SBP) for their function[11,12]. In Gram-positive bacteria and archaea, the SBPs are attached to the membrane via a lipid- or protein anchor, or are directly fused to the TMDs[13,14]. In Gram-negative bacteria, most SBPs are present as soluble protein in the periplasmic space, but some are lipid-anchored[15] or tethered to the TMD of the ABC transporter[16], which is analogous to the surface association of SBPs in Gram-positive bacteria and archaea. The SBP binds the transported substrate, i.e., the cognate substrate, for delivery to the translocator unit. SBPs share a domain architecture, consisting of two rigid subdomains connected by a flexible hinge region[11]. Binding of a cognate substrate brings the two subdomains together, thereby switching the SBP from an open to a closed conformation[17-19]. Different closed conformations can be formed with different cognate substrates[20]. These closed conformations productively interact with the translocator and activate transport and the ATPase activity[21-23].

Various biological compounds have been identified that bind to SBPs but are not transported by ABC importers[6,23-29]. These non-transported molecules are termed herein non-cognate substrates, whereas the molecules taken up are named cognate substrates. To date, non-cognate substrates have been identified for various ABC importers, including the maltose importer $MalFGK_2$ of *Escherichia coli*[29], the amino acid importer GlnPQ of *Lactococcus lactis*[20], the Mn^{2+} importer PsaBCA of *Streptococcus pneumoniae*[30], the osmoregulatory transporter OpuA of *L. lactis*[24], the peptide importer OppABCDF of *L. lactis*[27], the alginate importer AlgM1M2SS of *Sphingomonas sp.*[23] and the Zn^{2+} importer ZnuABC of *Salmonella typhimurium*[28]. The non-

cognate substrates can act as inhibitors of cognate substrate transport and thereby severely affect the transport rate *in vitro* and *in vivo*[20,25,28,29]. Note that this type of inhibition is distinct from trans-inhibition that exist in some ABC importers[31,32]. In the trans-inhibition mechanism the importer contains additional regulatory domains fused to the NBDs. Here, the activity of the transporter is regulated by the transported cognate substrate[31,32]. For instance, the transport of cognate L- and D-methionine by the *E. coli* MetINQ system is regulated by the internal pool of L-methionine[33].

Many non-cognate substrates induce a conformational change in the SBP that is distinct from that of cognate substrates[20,34,35]. For instance, the SBP MalE can bind maltotetraitol, β-cyclodextrin and maltotetraose with high affinity, but only maltotriose is transported[25]. Maltotriose induces closing of MalE, whereas maltotetraitol and β-cyclodextrin trigger the formation of different conformational states[20,34,35]. In other SBPs, the non-cognate substrate does not induce a conformational change within the SBP[20]. These observations provided possible explanations why the non-cognate substrate cannot be transported: the SBP-non-cognate substrate complex fails to interact with the translocator (model A, Figure 1) or it docks onto the translocator but fails to activate ATPase activity and transport (model B; Figure 1).

In the Mn^{2+} importer PsaBCA of *S. pneumoniae*, a third mechanism of substrate inhibition is prevalent[20,30]. Here, both cognate Mn^{2+} and non-cognate Zn^{2+} induce highly similar closing of the SBP PsaA. However, the PsaA-Zn^{2+} complex is so stable that PsaA cannot open and release the metal ion to the PsaBC unit (model C, Figure 1)[20,26,30,36]. Reversible and irreversible substrate binding has also been shown for YtgABC[37]. Thus, the rate of transport is not only influenced by the conformational state of the substrate-bound SBP but also by the substrate release kinetics.

In this paper, we used rate equations to analyse how non-cognate substrates influence the kinetics of transport. We considered three inhibition mechanisms of the non-cognate substrate that we here describe as model A, B and C. The most drastic differences between the models are found at saturating cognate and non-cognate substrate and saturating SBP concentrations. Then, the transport rate is not influenced by the non-cognate substrate in model A, the transport rate is partially reduced in model B, and transport is completely inhibited in model C. These findings show that the influence of the non-cognate substrate on the rate of cognate substrate transport depends crucially on its effect on the SBP.

Results

Model description

We modelled the transport cycle of an ABC importer by a minimal mathematical model based on available biochemical and structural data[1-3]. We focus on Type I ABC importers, as they are structurally and mechanistically different from other ABC importers[38]. We constructed four reaction schemes that model how a cognate substrate is transported, and how a non-cognate substrate interacts with the importer but is not transported (Figure 1). These models are termed model 0, A, B and C. The transport of cognate substrate is modelled in the absence of non-cognate substrate (model 0) and in its presence (model A, B and C). The difference between models A, B and C relates solely to how the non-cognate substrate is bound by the SBP and how the non-cognate substrate-SBP complex interacts with the translocator. The models consist of different states X_i, which are connected via rate constants k_j.

First, we describe the common steps of model 0, A, B and C, that are, the steps that involve the transport of cognate substrate (Figure 1). The first step is the reversible binding of cognate substrate X_6 to the open conformation of the SBP X_1 with an association and dissociation rate constant k_1 and k_2, respectively. Binding of the cognate substrate induces immediate closing of the SBP[19]. The substrate-free (open) and substrate-bound (closed) states of the SBP are denoted by X_1 and X_2, respectively. In our models, we ignore any other SBP states, such as a substrate-free closed or a substrate-bound open conformation, as these states represent only a very small fraction of the total SBP population and/or short-lived[19,20,39-42]. Next, the substrate-bound SBP docks onto the inward-facing conformation of the translocator with an association rate constant k_3. The formed complex is denoted X_3 and the free translocator X_5. Once docked on the translocator, the SBP can either undock (with a rate constant k_4) or transfer the cognate substrate to the TMDs (rate constant k_5). In this latter step, the SBP has to open and release the substrate into the TMD cavity of the outward-facing conformation[43]. The formed complex is denoted X_4. In the final step, ATP hydrolysis triggers formation of the inward-facing conformation and release of the cognate substrate into the cytoplasm. We assume that all these processes occur with rate constant k_6 in an irreversible process. By making the step with rate constant k_5 and k_6 irreversible, the transporter can only function in the import direction and it can only hydrolyse and not synthesise ATP. In our models we do not consider the proposed non-canonical mechanism of transport, in which SBP docking would precede substrate binding[44,45].

Next, we describe the additional steps of model A, B and C describing how a non-cognate substrate binds to the SBP and how the non-cognate substrate-SBP complex interacts with the importer (Figure 1). In model A (Figure 1), the non-cognate substrate X_7 binds to the open conformation of the SBP X_1 with an association and dissociation rate constant k_7 and k_8, respectively. The SBP with a non-cognate substrate bound is denoted by X_8. In model A, it is assumed that the non-cognate substrate does not trigger the correct conformational change in the

SBP[20,34,35] so that the SBP has no affinity for the translocator. Thus, the key characteristic of model A is that transport fails because the non-cognate substrate-SBP complex cannot dock onto the translocator. Model A is exemplified by the action of non-cognate substrates arginine and lysine of amino-acid importer GlnPQ, as these compounds leave the structure of SBD1 in the open conformation[20].

In model B (Figure 1), the non-cognate substrate is bound reversibly by the SBP with an association and dissociation rate constant k_7 and k_8, respectively. Contrary to model A, the non-cognate substrate-bound SBP can dock on to the translocator with an association and dissociation rate constant k_9 and k_{10}, respectively. The transport in model B, however, fails because the non-cognate substrate-SBP complex does not activate the translocator. We have previously shown that many non-cognate substrates induce a conformational change in the SBP that is distinct from those induced by cognate substrates[20,34,35]. Thus, transport fails because the required allosteric interactions between the SBP and TMD are not made. Potential examples of model B are the substrates histidine of GlnPQ and maltotetraitol and β-cyclodextrin of the *E. coli* maltose importer, which induce an SBP conformation that is different from that with cognate substrates[20,34,35].

Transport of non-cognate substrate fails in model C (Figure 1) because the non-cognate substrate binds irreversibly to the SBP (at least on any biologically relevant timescale). Irreversible substrate binding has been shown for the importers PsaBCA[20,30] and YtgABC[37]. In model C, the non-cognate substrate binds to the SBP with a rate constant k_7 and locks the SBP in the closed state. The SBP cannot open, so the substrate dissociation rate constant is equal to zero. After the complex between the non-cognate substrate and the SBP has been formed, it can dock onto the translocator with an association rate constant k_9. Next, the SBP can only undock again (with a rate constant k_{10}) but it cannot open and transfer the substrate to the translocator.

Comparing models

By using the law of mass action for each step of the reaction mechanism, we can formulate the equations that describe the time evolution of the concentrations of state X_j (see Supplementary Information for details). We calculated the steady-state transport rate of a single translocator of model i ($i \in \{0, A, B, C\}$):

$$v_i = \frac{k_6}{r} \cdot X_4^i \quad (1)$$

where X_4^i is the steady-state concentration of state X_4 of model i and r is the total translocator concentration. For model A, B and C, we calculated the steady-state transport rate relative to model 0:

$$j_i = \frac{v_i}{v_0} \tag{2}$$

where $i \in \{A, B, C\}$. The j_i value is indicative for the amount of inhibition by the non-cognate substrate: the transport rate of cognate substrate is not influenced by the presence of non-cognate substrate when $j_i = 1$, transport is completely inhibited when $j_i = 0$, and transport occurs with a reduced rate when $0 < j_i < 1$. Formally, v_i and j_i are functions of the rate constants, the total non-cognate substrate concentration L, the total cognate substrate concentration l, the total SBP concentration b, and the total translocator concentration r. However, for notational convenience we will omit this explicit dependence throughout this paper.

To compare the steady-state transport rates for the different models, we numerically solved the steady-state concentrations for a particular set of parameter values. We chose parameters that reflect known cases and typical assumptions and conditions of Type I importers. First, b was set to 20 µM and r to 1 µM, so that the SBP to translocator ratio is 20:1[46-49]. The rate constants k_1 and k_7 were set to 10 s^{-1} μM^{-1} and k_2 and k_8 to 10 s^{-1}, thereby fixing the cognate and non-cognate dissociation constant K_D to 1 µM[21,29]. The rate constants k_3 and k_9 were set to 1 s^{-1} μM^{-1} and k_4 to 10 s^{-1} and k_{10} to 20 s^{-1}, thereby fixing the K_D between the SBP and the translocator to 10 µM when the SBP has a cognate substrate bound and to 20 µM when a non-cognate substrate is bound[48,50-52]. We chose k_5 and k_2 to be equal, because both steps involve the opening of the SBP and release of substrate. Finally, k_6 was set to 4 s^{-1}, so that the maximal turnover rate is $k_5k_6/(k_5+k_6) \approx 3$ s^{-1} [14]. Unless stated otherwise, we used these rate constants throughout this paper.

Figure 2 shows v_i for a total cognate substrate concentration between 0 and 60 µM and in the presence and absence of 15 µM non-cognate substrate. We observe that v_0 increases with cognate substrate and approaches a maximum at high concentrations. This behaviour is also commonly observed experimentally[21]. In the presence of 15 µM of non-cognate substrate, we see that the amount of inhibition is model dependent. Transport is most severely inhibited when the non-cognate substrate binds irreversibly to the SBP (model C). Inhibition is the least when the non-cognate substrate binds reversibly and the non-cognate substrate-bound SBP cannot dock onto the translocator (model A). This conclusion seems to hold for every cognate substrate concentration, however, at low concentrations the difference between the models becomes smaller or even disappears when the concentration approaches zero (see Section 'Low substrate concentration'). To put it more formally, Figure 2 shows that $j_A \geq j_B \geq j_C$ irrespective of the precise cognate substrate concentration.

To analyse if this conclusion depends on the particular choice of model parameters, such as the total SBP concentration or the rate constants, we compared a large set of j_A, j_B and j_C values, which were calculated with random model parameters (details in Supplementary Information). The model parameters (i.e., the rate constants and L, l, b and r) were randomly drawn from a broad distribution. In total, $8{\cdot}10^4$ random model parameter combinations were used to calculate j_A, j_B and j_C. In Figure 3, the histograms for the resulting (j_A, j_B), (j_B, j_C) and (j_A, j_C) pairs are shown. We observe that the amount of inhibition in model A is always less than or equal to model B and C ($j_A \geq j_B$ and $j_A \geq j_C$), and that the inhibition in model B is always less than or equal to model C ($j_B \geq j_C$) (Figure 3). Therefore, we conclude that: $j_A \geq j_B \geq j_C$ irrespective of the rate constants or protein and substrate concentrations. Secondly, we see with certain model parameter combinations that transport is not influenced by the presence of non-cognate substrate ($j_i = 1$). Thirdly, with certain model parameter combinations, drastic differences are observed between model A, B and C, e.g., $j_A = 1$ and $j_B = 0$. These cases will be analysed in more detail in the next sections.

For simplicity, we treated many of the downstream steps of the transport cycle as a single step. To rule out that the conclusions depend on this oversimplification, we also considered several alternative model topologies, in which an additional step is included after substrate transfer to the TMDs (Figure S1a-c), the cognate substrate is translocated across the membrane before the SBP undocks (Figure S2a-c) or the SBP undocks before the cognate substrate is translocated (Figure S3a-c). Random parameter combinations were simulated and we find that the conclusions for the models of Figure 1 are also valid for the alternative model topologies (compare Figure 3 with Figure S1d, Figure S2d and Figure S3d). This suggests that our conclusions are not strictly model dependent.

Low substrate concentration

When both cognate and non-cognate substrate concentrations are low compared to the SBP and translocator concentration, then we can make the approximation that $b = X_1^i$ and $r = X_5^i$, where X_j^i is the steady-state concentration of state X_j of model i. With this approximation, the models can be solved analytically under steady-state conditions (see Supplementary Information). We find that the transport rate for model i is equal to

$$v_i = \frac{k_{1356} bl}{k_{246} + k_{256} + (k_{146} + k_{156})b + (k_{135} + k_{136})br + k_{356} r} \qquad (3)$$

where $i \in \{0, A, B, C\}$ and $k_{xyz} = k_x k_y k_z$. The v_i's calculated with Eq. 3 are in good agreement with the numerical solution, which do not rely on any approximation (Figure 4). The fact that v_0,

v_A, v_B and v_C are equal at low substrate concentrations, implies that j_A, j_B and j_C approaches the limit

$$j_A = j_B = j_C = 1 \tag{4}$$

Thus, when the non-cognate substrate concentration is much higher than the cognate substrate concentration, but both are low compared to the protein concentrations, transport is not inhibited in model A, B and C. Since the typical translocator and SBP concentrations are in the μM-mM range[46-49], the result of Eq. 4 should apply when the cognate and non-cognate substrates are present in sub-μM concentrations or lower, which is not uncommon for bacteria in e.g. marine environments and may evoke a selective advantage on expressing SBP at high levels.

High substrate concentration

Next, we analysed the situation that the substrates are available to the SBP at saturating concentrations (i.e. $l \gg b$ and $L \gg b$) and the SBP is present in large excess of the translocator concentration (i.e. $b \gg r$). The first condition is important for ABC importers in bacteria that are (transiently) exposed to high nutrient concentrations such as gut microbiota and enterobacteriaceae[46-49,53]. In a subset of ABC transporters (abundantly present in firmicutes), multiple SBPs are directly linked to the importer, giving rise to more than one SBP per transporter complex[13]. Under the here analysed conditions, all free SBPs have a cognate or non-cognate substrate bound and the majority of translocators have an SBP bound. Simple analytical results can be obtained in this case (see Supplementary Information). To ensure that all limits of this section exist we only look at $0 < L/l < \infty$, where L/l is the ratio of non-cognate substrate over cognate substrate concentration.

The steady-state transport rate in the absence of non-cognate substrate is

$$v_0 = \frac{k_{356} b}{k_{46} + k_{56} + (k_{35} + k_{36}) b} \tag{5}$$

and in the presence of non-cognate substrate,

$$v_A = \frac{k_{13568} bl}{(k_{1358} + k_{1368}) bl + (k_{1468} + k_{1568}) l + (k_{2467} + k_{2567}) L} \tag{6}$$

$$v_B = \frac{k_{13568} bl}{\left((k_{1358} + k_{1368}) bl + (k_{1468} + k_{1568}) l + (k_{2467} + k_{2567}) L\right) + \frac{(k_{24679} + k_{25679})}{k_{10}} bL} \tag{7}$$

and

$$v_C = 0 \tag{8}$$

By using Eq. 6, 7 and 8, we calculated the transport rate at high substrate concentrations and with a total SBP and translocator concentration of 25 and 0.5 μM, respectively. We see that the rates calculated with Eq. 6, 7 and 8 are in good agreement with the numerical solution, in which no approximations are made (Figure 5a).

To gain more insight in the amount of inhibition for each non-cognate interaction mechanism, we determined the transport rate relative to v_0,

$$j_A = \frac{v_A}{v_0} = \frac{(k_{1468} + k_{1568})l + (k_{1358} + k_{1368})bl}{(k_{1358} + k_{1368})bl + (k_{1468} + k_{1568})l + (k_{2467} + k_{2567})L} \tag{9}$$

$$j_B = \frac{v_B}{v_0} = \frac{(k_{1468} + k_{1568})l + (k_{1358} + k_{1368})bl}{\left((k_{1358} + k_{1368})bl + (k_{1468} + k_{1568})l + (k_{2467} + k_{2567})L\right) + \frac{(k_{24679} + k_{25679})}{k_{10}}bL} \tag{10}$$

and

$$j_C = \frac{v_C}{v_0} = 0 \tag{11}$$

From Eq. 9, 10 and 11 we conclude that transport still occurs when the non-cognate substrate binds reversibly to the SBP (model A and B). In contrast, irreversible binding (model C) completely inhibits transport under these conditions (see also Figure 5a). The interpretation of this result is simple. When the non-cognate substrate concentration is higher than the SBP concentration ($L > b$) and the binding is irreversible, all the SBPs have a non-cognate substrate bound, so that no SBPs are available for transport. In model A and B, only a fraction of the SBPs have a non-cognate substrate bound, so leaving the others free to participate in transport.

From Eq. 9 and Eq. 10 we see that when the cognate substrate concentration becomes much larger than the non-cognate substrate concentration, we have that $j_A \to 1$ and $j_B \to 1$. However, this is not true for j_C, unless the non-cognate substrate concentration is negligible compared to the SBP and translocator concentration (see Section 'Low substrate concentration'). These observations are consistent with the expected non-competitive inhibition mode for model C and competitive inhibition mode for model A and B.

Next, we analyse how j_A and j_B (as given by Eq. 9 and 10, respectively) depend on the total SBP concentration; a variable that might be adjusted by the cell[49]. In Figure 5b, j_A is shown for different SBP concentrations. We observe that the amount of inhibition decreases with increasing

SBP concentration (Figure 5b). When the translocator becomes saturated with SBP (Figure 5c), then the following limit is obtained

$$j_A = 1 \tag{12}$$

This means that transport becomes insensitive to non-cognate substrate. This conclusion is valid irrespective of the rate constants and the substrate, SBP and translocator concentration, as long as the substrates and SBPs are both present at saturating levels.

By using Eq. 10 we calculated j_B for different SBP concentrations (Figure 5d). We see that contrary to model A, an intermediate value of j_B is obtained when the translocators are saturated with SBP (Figure 5d-e). From Eq. 10 it follows that at high SBP concentrations, j_B approaches the limit

$$j_B = \frac{K}{K + L/l} \tag{13}$$

where

$$K = \frac{k_{13810}(k_{-} + \kappa_6)}{k_{2679}(k_{-} + l_{-5})} \tag{14}$$

Eq. 13 and 14 show that the extent of inhibition depends on the rate constants and the ratio L/l. Thus, in the presence of a high SBP concentration, the non-cognate substrate inhibits transport in model B, but not in model A. In conclusion, the different non-cognate interaction mechanisms have a radically different influence on the inhibition of transport, ranging from a complete inhibition in model C to a complete preservation of transport in model A.

Discussion

ABC importers constitute major uptake pathways of prokaryotes, and Type I and Type II importers require an extra-cytoplasmic SBP for function[11]. Various compounds have been identified that are bound by SBPs but that cannot be transported by the corresponding ABC importer[6,23-28]. Most of the examined non-cognate substrates induce an SBP conformation that is different from the conformation that is formed with cognate substrates[20,34,35]. Thus, transport can fail because the non-cognate substrate-SBP complex cannot dock onto the TMD or the docked SBP cannot provide the signal for transport activation (Figure 1). Other non-cognate substrates lock the SBP in the closed state and transport fails because the SBP cannot transfer the substrate to the translocator[20,30]. We cannot rule out that other non-cognate substrate interaction mechanisms exist. For instance, in certain ABC importers non-cognate substrates might directly affect the transport by binding to cavities within the membrane domain. In $MalFGK_2$[54] from *E.*

coli and Art(QM)$_2$[55] from *Thermoanaerobacter tengcongensi* substrate-binding pockets have been identified inside the TMDs. Similar solvent-filled cavities within the TMDs have not been observed in the high-resolution structures of other ABC importers[56-58], although pockets through which the substrate passes in the transition of the TMD from outward- to inward-facing must be present. The binding pockets within the TMDs have been linked to the regulation of transport[59,60], however, we believe that further molecular details are required to model these interaction mechanisms. For instance, it is unknown how a trapped non-cognate substrate is removed from the binding pockets of the TMDs and how the importer resets to its resting state.

Here, we used rate equations to model different non-cognate SBP-interaction mechanisms and analysed their effect on the steady-state transport rate. We conclude that when the same substrate, SBP and translocator concentrations and the common set of rate constants are used, a hierarchy in the extent of inhibition exists among the models (Figures 3). More specifically, inhibition is most severe when the non-cognate substrate binds irreversibly to the SBP (model C; Figure 1). Inhibition is less prominent, when the binding is reversible and the SBP with a non-cognate substrate bound can dock onto the translocator (model B; Figure 1). When the binding is reversible, but the SBP with a non-cognate substrate bound cannot dock (model A; Figure 1), then the extent of inhibition is the least of all three mechanisms. In model A only a fraction of the total SBP population is effectively taken out by the binding of non-cognate substrate. In model B, the non-cognate substrate-bound SBP can dock onto the translocator, so only a fraction of both the SBP and translocator population is effectively taken out by the non-cognate substrate. This explains why transport in model B is always slower than in model A. In model C, the non-cognate substrate binds irreversibly, and more SBPs have a non-cognate substrate bound than in model B. Therefore, the SBPs that can effectively participate in transport is reduced even further in model C when compared to model B.

Analytical results were obtained in the presence of low and high substrate concentrations (Section 'Low substrate concentration' and 'High substrate concentration', respectively). We observe that transport in model A, B and C is not influenced by the non-cognate substrate when both cognate and non-cognate substrates are present at low concentrations (Figure 4). When the non-cognate substrate concentration is well below the SBP and translocator concentration, then these protein concentrations can only be changed by an amount that is smaller than the non-cognate substrate concentration, which in this limit is negligible when compared to the total protein concentrations. The conclusion holds irrespective of the rate constants. Thus, it should even apply when different cognate and/or non-cognate substrates are compared. For example, the non-cognate substrates arginine and lysine have in common that they do not trigger closing of SBD1 and both inhibit glutamine and asparagine transport via GlnPQ[20]. However, the K_D of

arginine binding by SBD1 is more than one order of magnitude lower than that of lysine[20]. This implies that also their association (k_7) and/or dissociation (k_8) rate constants are different, because $K_D = k_8/ k_7$. Since Eq. 3 is independent of these rate constants, their effect on transport is the same, i.e., transport of glutamine and asparagine by GlnPQ is not inhibited at low concentrations of arginine and lysine. These predictions can be verified experimentally, by performing uptake assays at substrate concentrations that are below the SBP and translocator concentration.

Contrary to the inhibition at low substrate concentrations, the different non-cognate interaction mechanisms inhibit transport completely differently in the limit that the non-cognate and cognate substrates and SBPs are present at saturating concentrations (see Eq. 11, 12 and 13). In this limit, transport is completely inhibited in model C, but not in model A and B. Interestingly, transport in model A is unaffected by the presence of non-cognate substrate, even if the concentration is much higher than that of the cognate substrate. In contrast, transport is inhibited in model B, with an amount that depends on the rate constants and the cognate and non-cognate substrate concentrations. The interpretation of this result is simple. First, when the non-cognate substrate binds irreversibly to the SBP and the non-cognate substrate concentration is higher than the SBP concentration, then the SBPs are saturated with non-cognate substrate, and SBPs are no longer available for transport. In model A and B, the binding is reversible, so an SBP contains either a cognate or non-cognate substrate. In model B, the SBPs with a cognate substrate compete for docking onto the translocator with the SBPs that have a non-cognate substrate bound, thereby causing partial inhibition of transport. In model A, these SBPs do not compete, so that transport becomes unaffected by the presence of non-cognate substrate. These conclusions hold irrespective of the rate constants and should therefore even apply when different cognate and/or non-cognate substrates are compared.

In conclusion, the different mechanisms of substrate inhibition have strongly varying impact on the transport kinetics of ABC importers, which might explain how prokaryotes maintain efficient uptake in chemical diverse external environments and might contribute to the development of effective inhibitors against SBPs of pathogenic bacteria.

Methods

The system of nonlinear equations was numerically solved with the software package MATLAB (MathWorks). The solution was iteratively found using the Trust Region method together with the Dogleg approach, as implemented in the *fsolve* function. Default settings of the *fsolve* function were used, except for certain thresholds of convergence. Convergence was reached when the change in the solution and/or the objective function between two subsequent iterations was

smaller than 10^{-12} -10^{-14}. The initial conditions were varied in case no convergence was reached. The source code for the numerical calculations is available at a dedicated GitHub repository (https://github.com/MJdeBoer/Kinetic_model). Exact solutions were found with the software package Mathematica (WolframAlpha). Equations and derivations are provided in the Supplementary Information.

Acknowledgements

This work was financed by an ERC starting grant (SM-IMPORT; #638536 to TC) and an ERC Advanced Grant (ABCVolume; #670578 to BP). We thank Monique Wiertsema, Douglas Griffith and Erik van der Giessen for discussions and suggestions.

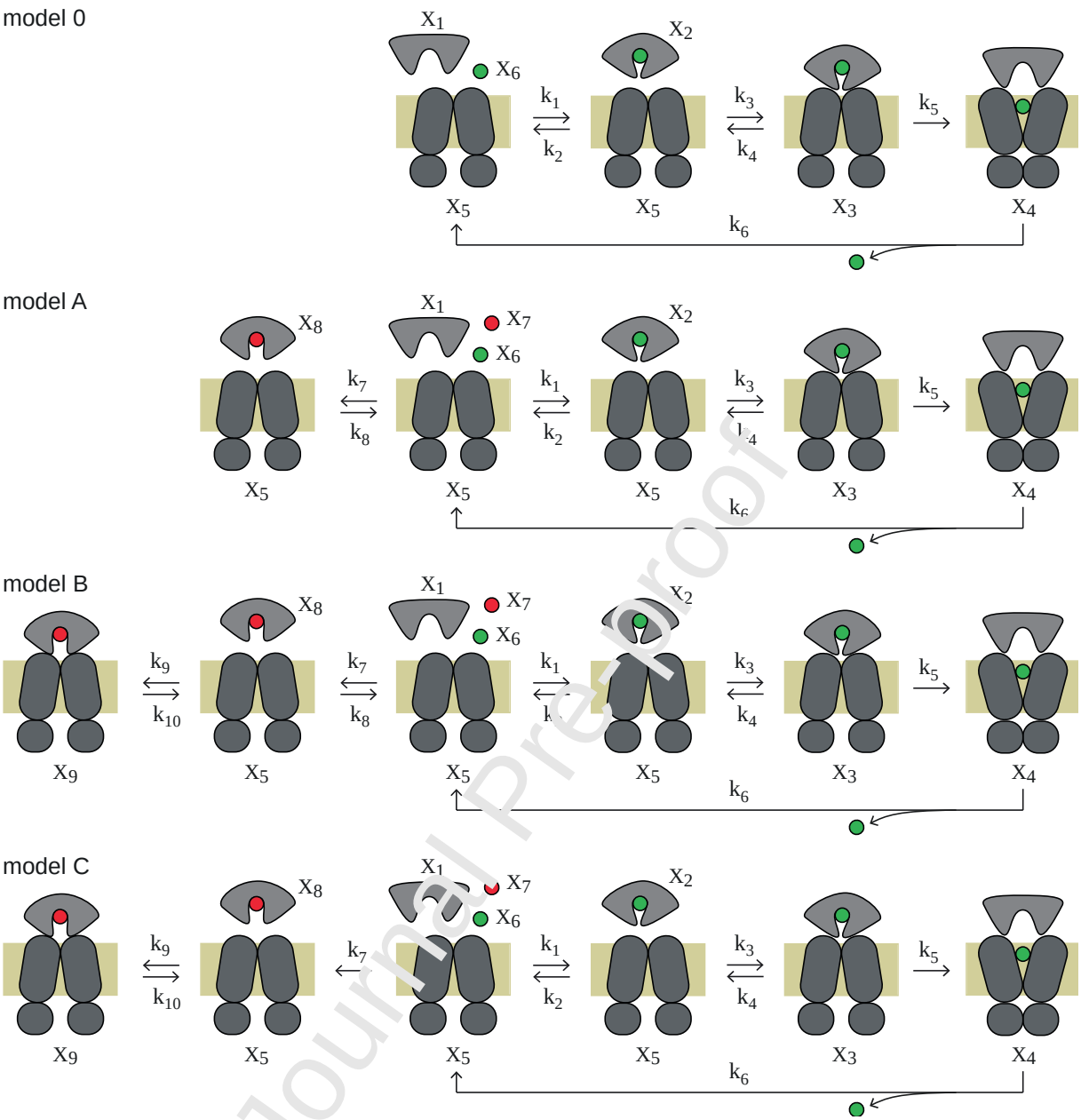

Figure 1. Transport mode of Type I ABC importers. Reaction scheme of model 0, A, B and C. Rate constants are denoted above the arrows and the states X_j are depicted as cartoon. The cognate and non-cognate substrates are shown in green and red, respectively. The SBP is depicted in light grey and the translocator in dark grey. Details of the models are described in the main text.

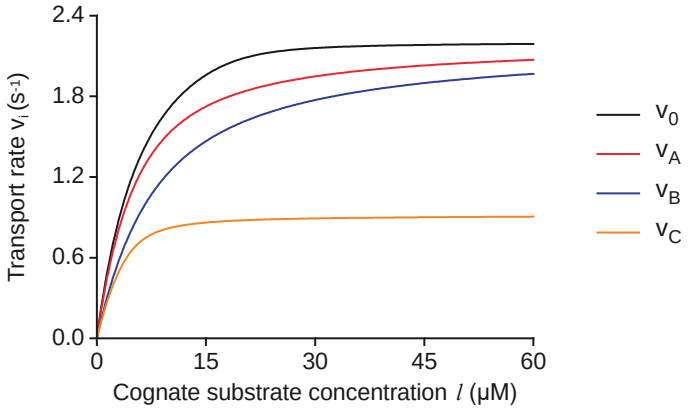

Figure 2. Transport rate in the presence and absence of non-cognate substrate. Numerical calculation of the steady-state transport rate in the absence of non-cognate substrate (model 0; black line) and in the presence of a total non-cognate substrate concentration of L = 15 μM for model A (red line), B (blue line) and C (yellow line) at various total cognate substrate concentrations l is shown. The total SBP (b) and total translocator (r) concentration are 20 and 1 μM, respectively.

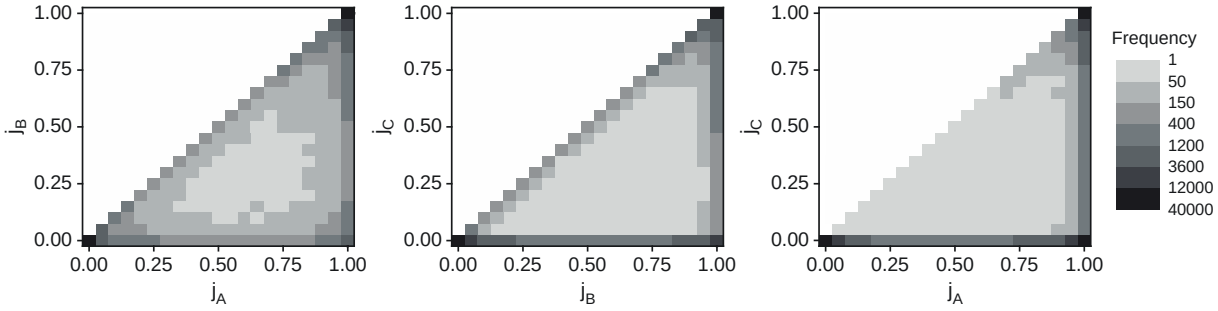

Figure 3. Normalized transport rate for model A, B and C with random model parameters. A set of model parameters that consist of the rate constants and the total cognate substrate, non-cognate substrate, SBP, and translocator concentration were randomly drawn from a broad distribution. For each set of random model parameters the j_B, j_C and j_D values were calculated. A total of $8{\cdot}10^4$ of random model parameters combinations were tested. The resulting histograms for the (j_A, j_B), (j_B, j_C) and (j_A, j_C) pairs are presented in the figure, with the grey-scale indicating the frequency of occurrence. See the Supplementary Information for further details about the sampling procedure.

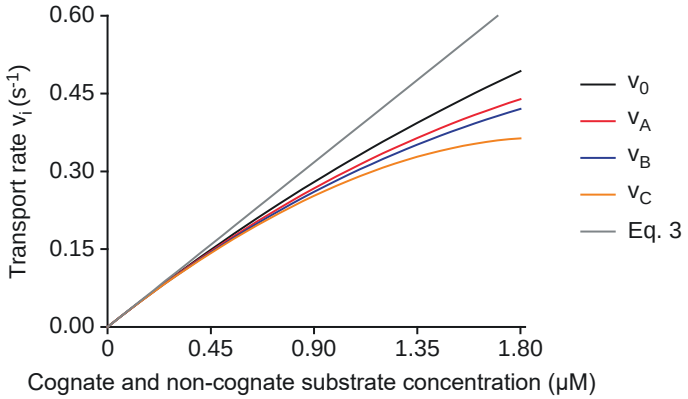

Figure 4. Transport at low substrate concentrations. Numerical calculation of the steady-state transport rate in the absence of non-cognate substrate (model 0; black line) and in the presence of non-cognate substrate for model A (red line), B (blue line) and C (yellow line) at various cognate and non-cognate substrate concentrations. The grey line denotes the analytic result of Eq. 3. In the calculation, the cognate (l) and non-cognate (L) substrate concentration are equal (l = L). The total SBP (b) and total translocator (r) concentrations are 4 and 1 μM, respectively. The rate constants were used as described in the Section 'Model description'.

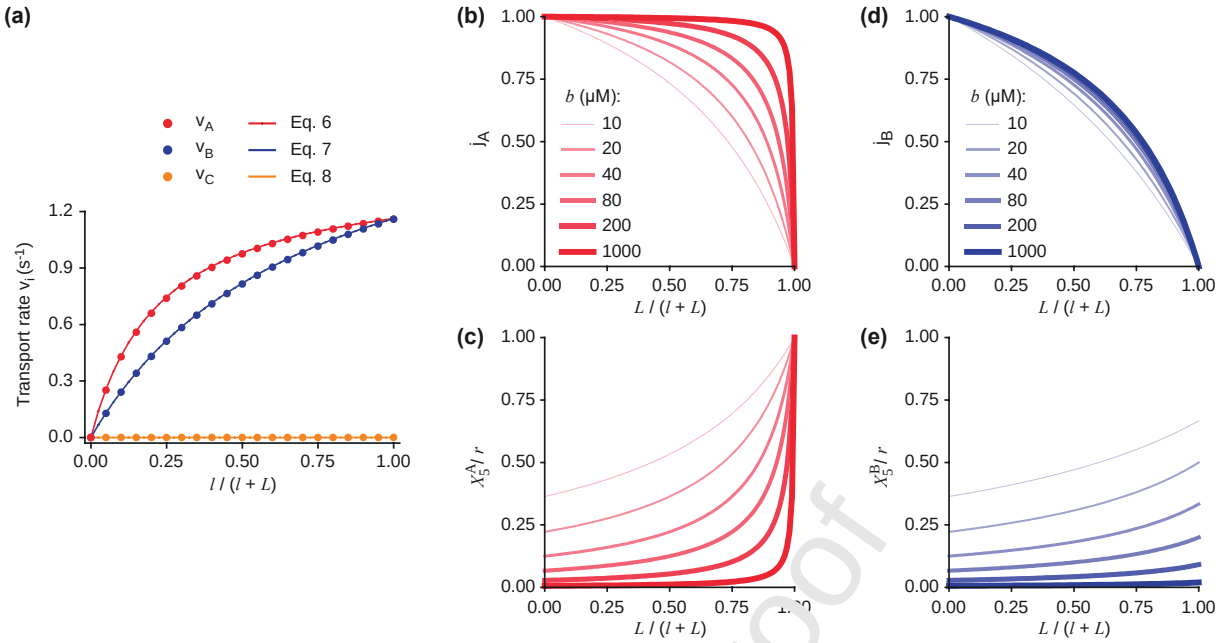

Figure 5. Transport at high substrate and high SBP concentrations. (a) Steady-state transport rate for model A (red), B (blue) and C (yellow) as function of the relative cognate substrate concentration $l/(l+L)$, where L and l are the total non-cognate and cognate substrates concentrations, respectively. The total SBP (b) and total translocator (r) concentrations are 25 and 0.5 μM, respectively. The continuous line denotes the numerical solution with no approximations made and the points are the transport rate calculated with Eq. 6, 7 and 8 as indicated. The normalized steady-state transport rate as a function of the relative non-cognate substrate concentration $L/(l+L)$ and various SBP concentrations for model A **(b)** and B **(d)** calculated with Eq. 9 and 10. Relative population of the free translocator state X_5^A/r **(c)** and X_5^B/r **(e)** as function of the relative non-cognate substrate concentration and various SBP concentrations. In all the calculations of this figure the total substrate (l + L) was equal to 100 mM. The rate constants were used as described in the Section 'Model description'.

References

1. Higgins CF. ABC transporters: From microorganisms to man. *Annu Rev Cell Biol*. 1992;8:67-113.

2. Davidson AL, Dassa E, Orelle C, Chen J. Structure, function, and evolution of bacterial ATP-binding cassette systems. *Microbiol Mol Biol Rev*. 2008;72(2):317-64, table of contents.

3. Locher KP. Mechanistic diversity in ATP-binding cassette (ABC) transporters. *Nat Struct Mol Biol*. 2016;23(6):487-493.

4. Husada F, Bountra K, Tassis K, et al. Conformational dynamics of the ABC transporter McjD seen by single-molecule FRET. *EMBO J*. 2018;37(21):10.15252/embj.2018100056. Epub 2018 Sep 20.

5. Li Y, Yuan H, Yang K, Xu W, Tang W, Li X. The structure and functions of P-glycoprotein. *Curr Med Chem*. 2010;17(8):786-800.

6. Ferenci T. The recognition of maltodextrins by escherichia coli. *Eur J Biochem*. 1980;108(2):631-636.

7. Higgins CF, Linton KJ. The ATP switch model for ABC transporters. *Nat Struct Mol Biol*. 2004;11(10):918-926.

8. Jardetzky O. Simple allosteric model for membrane pumps. *Nature*. 1966;211(5052):969-970.

9. Kang J, Hwang JU, Lee M, et al. PDR-type ABC transporter mediates cellular uptake of the phytohormone abscisic acid. *Proc Natl Acad Sci U S A*. 2010;107(5):2355-2360.

10. Rempel S, Gati C, Nijland M, et al. A mycobacterial ABC transporter mediates the uptake of hydrophilic compounds. *Nature*. 2020;580(7803):409-412.

11. Berntsson RP, Smits SH, Schmitt L, Slotboom DJ, Poolman B. A structural classification of substrate-binding proteins. *FEBS Lett*. 2010;584(12):2606-2617.

12. Scheepers GH, Lycklama A Nijeholt JA, Poolman B. An updated structural classification of substrate-binding proteins. *FEBS Lett*. 2016;590(23):4393-4401.

13. van der Heide T, Poolman B. ABC transporters: One, two or four extracytoplasmic substrate-binding sites? *EMBO Rep*. 2002;3(10):938-943.

14. Schuurman-Wolters GK, de Boer M, Pietrzyk MK, Poolman B. Protein linkers provide limits on the domain interactions in the ABC importer GlnPQ and determine the rate of transport. *J Mol Biol*. 2018;430(8):1249-1262.

15. Carlson ML, Stacey RG, Young JW, et al. Profiling the escherichia coli membrane protein interactome captured in peptidisc libraries. *Elife*. 2019;8:10.7554/eLife.46615.

16. Licht A, Bommer M, Werther T, Neumann K, Hobe C, Schneider E. Structural and functional characterization of a maltose/maltodextrin ABC transporter comprising a single solute binding domain (MalE) fused to the transmembrane subunit MalF. *Res Microbiol*. 2019;170(1):1-12.

17. Quiocho FA, Ledvina PS. Atomic structure and specificity of bacterial periplasmic receptors for active transport and chemotaxis: Variation of common themes. *Mol Microbiol*. 1996;20(1):17-25.

18. Shilton BH, Flocco MM, Nilsson M, Mowbray SL. Conformational changes of three periplasmic receptors for bacterial chemotaxis and transport: The maltose-, glucose/galactose- and ribose-binding proteins. *J Mol Biol*. 1996;264(2):350-363.

19. de Boer M, Gouridis G, Muthahari YA, Cordes T. Single-molecule observation of ligand binding and conformational changes in FeuA. *Biophys J*. 2019;117(9):1642-1654.

20. de Boer M, Gouridis G, Vietrov R, et al. Conformational and dynamic plasticity in substrate-binding proteins underlies selective transport in ABC importers. *Elife*. 2019;8:10.7554/eLife.44652.

21. Gouridis G, Schuurman-Wolters GK, Ploetz E, et al. Conformational dynamics in substrate-binding domains influences transport in the ABC importer GlnPQ. *Nat Struct Mol Biol*. 2015;22(1):57-64.

22. Orelle C, Ayvaz T, Everly RM, Klug CS, Davidson AL. Both maltose-binding protein and ATP are required for nucleotide-binding domain closure in the intact maltose ABC transporter. *Proc Natl Acad Sci U S A*. 2008;105(35):12837-12842.

23. Kaneko A, Uenishi K, Maruyama Y, et al. A solute-binding protein in the closed conformation induces ATP hydrolysis in a bacterial ATP-binding cassette transporter involved in the import of alginate. *J Biol Chem*. 2017;292(38):15681-15690.

24. Wolters JC, Berntsson RP, Gul N, et al. Ligand binding and crystal structures of the substrate-binding domain of the ABC transporter OpuA. *PLoS One*. 2010;5(4):e10361.

25. Hall JA, Ganesan AK, Chen J, Nikaido H. Two modes of ligand binding in maltose-binding protein of escherichia coli. functional significance in active transport. *J Biol Chem*. 1997;272(28):17615-17622.

26. McDevitt CA, Ogunniyi AD, Valkov E, et al. A molecular mechanism for bacterial susceptibility to zinc. *PLoS Pathog*. 2011;7(11):e1002357.

27. Charbonnel P, Lamarque M, Piard JC, Gilbert C, Juillard V, Atlan D. Diversity of oligopeptide transport specificity in lactococcus lactis species. A tool to unravel the role of OppA in uptake specificity. *J Biol Chem*. 2003;278(17):14832-14840.

28. Ilari A, Pescatori L, Di Santo R, et al. Salmonella enterica serovar typhimurium growth is inhibited by the concomitant binding of zn(II) and a pyrrolyl-hydroxamate to ZnuA, the soluble component of the ZnuABC transporter. *Biochim Biophys Acta*. 2016;1860(3):534-541.

29. Ferenci T, Muir M, Lee KS, Maris D. Substrate specificity of the escherichia coli maltodextrin transport system and its component proteins. *Biochim Biophys Acta*. 1986;860(1):44-50.

30. Counago RM, Ween MP, Begg SL, et al. Imperfect coordination chemistry facilitates metal ion release in the psa permease. *Nat Chem Biol*. 2014;10(1):35-41.

31. Gerber S, Comellas-Bigler M, Goetz BA, Locher KP. Structural basis of trans-inhibition in a molybdate/tungstate ABC transporter. *Science*. 2008;321(5886):246-250.

32. Yang JG, Rees DC. The allosteric regulatory mechanism of the escherichia coli MetNI methionine ATP binding cassette (ABC) transporter. *J Biol Chem*. 2015;290(14):9135-9140.

33. Kadner RJ. Regulation of methionine transport activity in escherichia coli. *J Bacteriol*. 1975;122(1):110-119.

34. Hall JA, Thorgeirsson TE, Liu J, Shin YK, Nikaido H. Two modes of ligand binding in maltose-binding protein of escherichia coli. electron paramagnetic resonance study of ligand-induced global conformational changes by site-directed spin labeling. *J Biol Chem*. 1997;272(28):17610-17614.

35. Skrynnikov NR, Goto NK, Yang D, et al. Orienting domains in proteins using dipolar couplings measured by liquid-state NMR: Differences in solution and crystal forms of maltodextrin binding protein loaded with beta-cyclodextrin. *J Mol Biol*. 2000;295(5):1265-1273.

36. Lawrence MC, Pilling PA, Epa VC, Berry AM, Ogunniyi AD, Paton JC. The crystal structure of pneumococcal surface antigen PsaA reveals a metal-binding site and a novel structure for a putative ABC-type binding protein. *Structure*. 1998;6(12):1553-1561.

37. Luo Z, Neville SL, Campbell R, et al. Structure and metal binding properties of chlamydia trachomatis YtgA. *J Bacteriol*. 2019;202(1):10.1128/JB.00580-19. Print 2019 Dec 6.

38. Swier LJYM, Slotboom DJ, Poolman B. ABC transporters: A structure-function perspective. In: George AM, ed. *ABC transporters - 40 years on.* 1st ed. Springer International Publishing; 2016:3-36. 10.1007/978-3-319-23476-2.

39. Van Meervelt V, Soskine M, Singh S, et al. Real-time conformational changes and controlled orientation of native proteins inside a protein nanoreactor. *J Am Chem Soc*. 2017;139(51):18640-18646.

40. Tang C, Schwieters CD, Clore GM. Open-to-closed transition in apo maltose-binding protein observed by paramagnetic NMR. *Nature*. 2007;449(7165):1078-1082.

41. Kim E, Lee S, Jeon A, et al. A single-molecule dissection of ligand binding to a protein with intrinsic dynamics. *Nat Chem Biol*. 2013;9(5):313-318.

42. de Boer M. The relation between intrinsic protein conformational changes and ligand binding. *bioRxiv* 974634 [Preprint], doi: https://doi.org/10.1101/2020.03.03.974634

43. Oldham ML, Khare D, Quiocho FA, Davidson AL, Chen J. Crystal structure of a catalytic intermediate of the maltose transporter. *Nature*. 2007;450(7169):515-521.

44. Bao H, Duong F. Discovery of an auto-regulation mechanism for the maltose ABC transporter MalFGK2. *PLoS One*. 2012;7(4):e34836.

45. Nguyen PT, Lai JY, Lee AT, Kaiser JT, Rees DC. Noncanonical role for the binding protein in substrate uptake by the MetNI methionine ATP binding cassette (ABC) transporter. *Proc Natl Acad Sci U S A*. 2018;115(45):E10596-E10604.

46. Li GW, Burkhardt D, Gross C, Weissman JS. Quantifying absolute protein synthesis rates reveals principles underlying allocation of cellular resources. *Cell*. 2014;157(3):624-635.

47. Hengge R, Boos W. Maltose and lactose transport in escherichia coli. examples of two different types of concentrative transport systems. *Biochim Biophys Acta*. 1983;737(3-4):443-478.

48. Ames GF, Liu CE, Joshi AK, Nikaido K. Liganded and unliganded receptors interact with equal affinity with the membrane complex of periplasmic permeases, a subfamily of traffic ATPases. *J Biol Chem*. 1996;271(24):14264-14270.

49. Schmidt A, Kochanowski K, Vedelaar S, et al. The quantitative and condition-dependent escherichia coli proteome. *Nat Biotechnol*. 2016;34(1):104-110.

50. Merino G, Boos W, Shuman HA, Bohl E. The inhibition of maltose transport by the unliganded form of the maltose-binding protein of escherichia coli: Experimental findings and mathematical treatment. *J Theor Biol*. 1995;177(2):171-179.

51. Vigonsky E, Ovcharenko E, Lewinson O. Two molybdate/tungstate ABC transporters that interact very differently with their substrate binding proteins. *Proc Natl Acad Sci U S A*. 2013;110(14):5440-5445.

52. Doeven MK, van den Bogaart G, Krasnikov V, Poolman B. Probing receptor-translocator interactions in the oligopeptide ABC transporter by fluorescence correlation spectroscopy. *Biophys J*. 2008;94(10):3956-3965.

53. Nigam SK, Bush KT. Uraemic syndrome of chronic kidney disease: Altered remote sensing and signalling. *Nat Rev Nephrol*. 2019;15(5):301-316.

54. Oldham ML, Chen S, Chen J. Structural basis for substrate specificity in the escherichia coli maltose transport system. *Proc Natl Acad Sci U S A*. 2013;110(45):18132-18137.

55. Yu J, Ge J, Heuveling J, Schneider E, Yang M. Structural basis for substrate specificity of an amino acid ABC transporter. *Proc Natl Acad Sci U S A*. 2015;112(16):5243-5248.

56. Woo JS, Zeltina A, Goetz BA, Locher KP. X-ray structure of the yersinia pestis heme transporter HmuUV. *Nat Struct Mol Biol*. 2012;19(12):1310-1315.

57. Pinkett HW, Lee AT, Lum P, Locher KP, Rees DC. An inward-facing conformation of a putative metal-chelate-type ABC transporter. *Science*. 2007;315(5810):373-377.

58. Locher KP, Lee AT, Rees DC. The E. coli BtuCD structure: A framework for ABC transporter architecture and mechanism. *Science*. 2002;296(5570):1091-1098.

59. Heuveling J, Landmesser H, Schneider E. One intact transmembrane substrate binding site is sufficient for the function of the homodimeric type I ATP-binding cassette importer for positively charged amino acids art(MP)2 of geobacillus stearothermophilus. *J Bacteriol*. 2018;200(12):10.1128/JB.00092-18. Print 2018 Jun 15.

60. Heuveling J, Landmesser H, Schneider E. Evidence from mutational analysis for a single transmembrane substrate binding site in the histidine ATP-binding cassette transporter of salmonella enterica serovar typhimurium. *J Bacteriol*. 2018;201(2):10.1128/JB.00521-18. Print 2019 Jan 15.

Research highlights:

- Receptors of ABC importers can bind a large variety of substrate but not all are transported

- Failure to transport a non-cognate substrate can be due to the receptor binding mechanism or the interaction of the receptor to the translocator unit of the ABC importer

- A kinetic model describes the different mechanisms by which non-cognate substrates are bound but not translocated

- Non-cognate substrates can affect the transport of cognate substrates in competitive or non-competitive manner

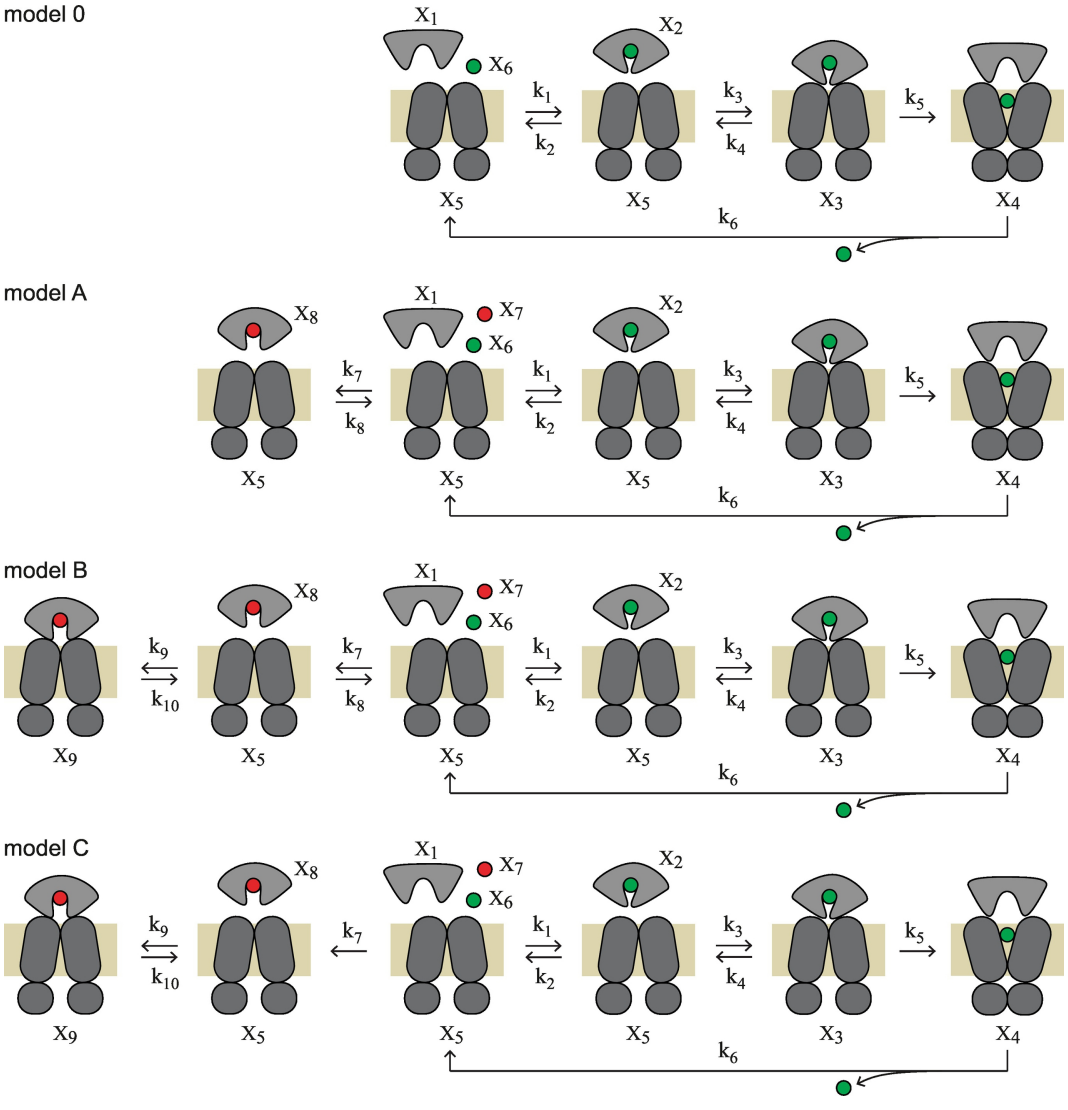
model 0
X1
X6
X2
k1
k2
k3
k4
k5
X5
X5
X3
X4
k6
model A
X8
X1
X7
X6
X2
k7
k8
k1
k2
k3
k4
k5
X5
X5
X5
X3
X4
k6
model B
X8
X1
X7
X6
X2
k9
k10
k7
k8
k1
k2
k3
k4
k5
X9
X5
X5
X5
X3
X4
k6
model C
X8
X1
X7
X6
X2
k9
k10
k7
k1
k2
k3
k4
k5
X9
X5
X5
X5
X3
X4
k6

Figure 1

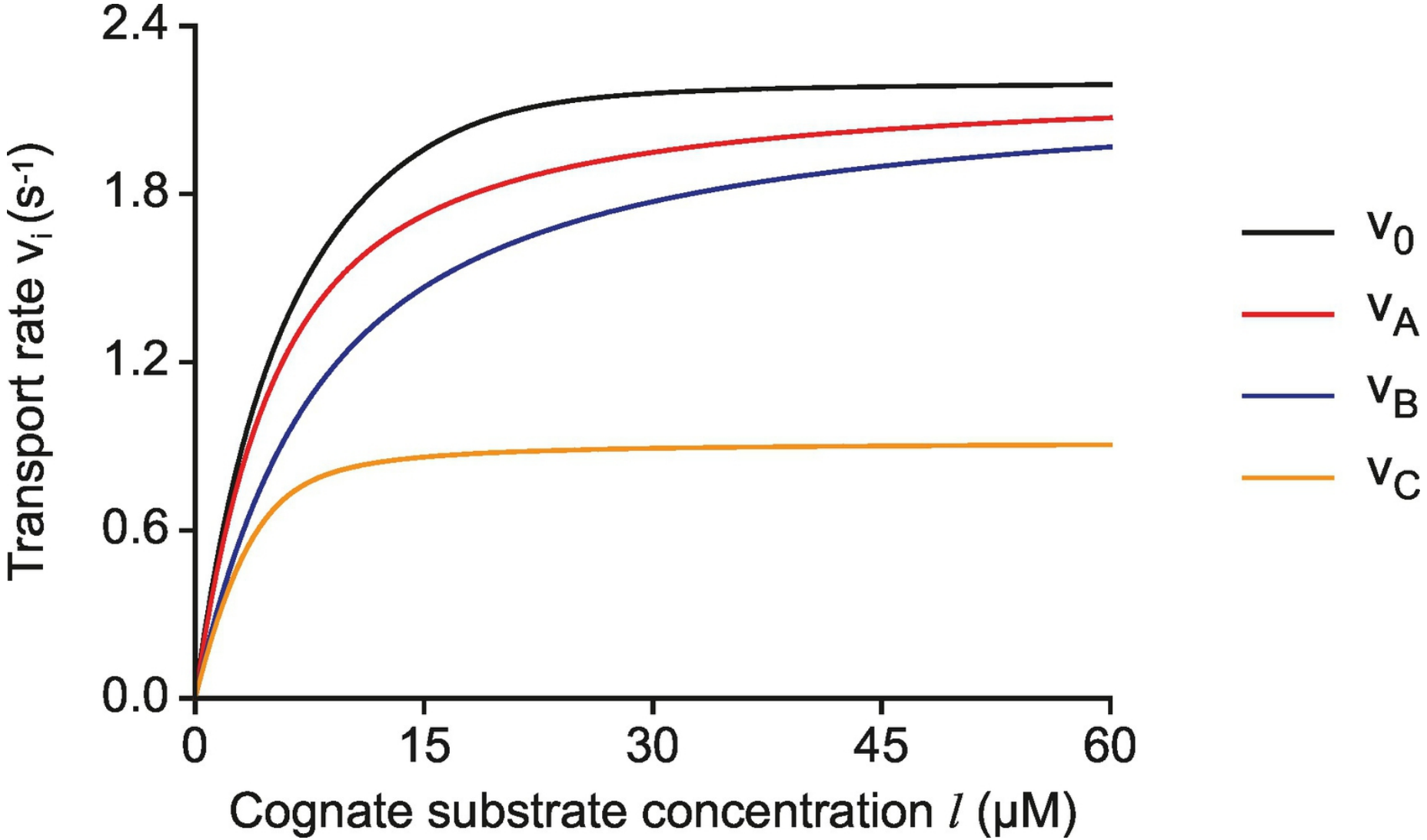
2.4
1.8
1.2
0.6
0.0
Transport rate v_i (s^{-1})
0
15
30
45
60
Cognate substrate concentration l (μM)
v_0
v_A
v_B
v_C

Figure 2

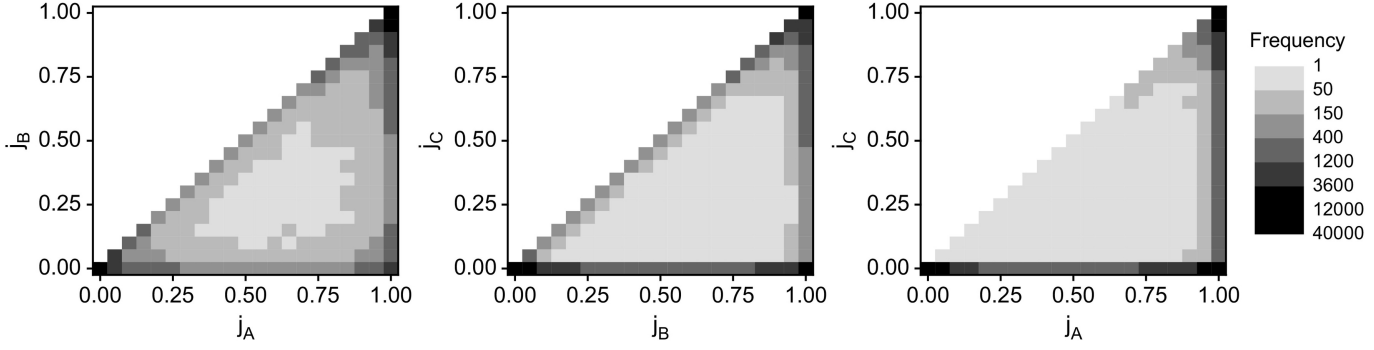
1.00
0.75
0.50
0.25
0.00
j_B
0.00 0.25 0.50 0.75 1.00
j_A
j_C
j_B
j_C
j_A
Frequency
1
50
150
400
1200
3600
12000
40000

Figure 3

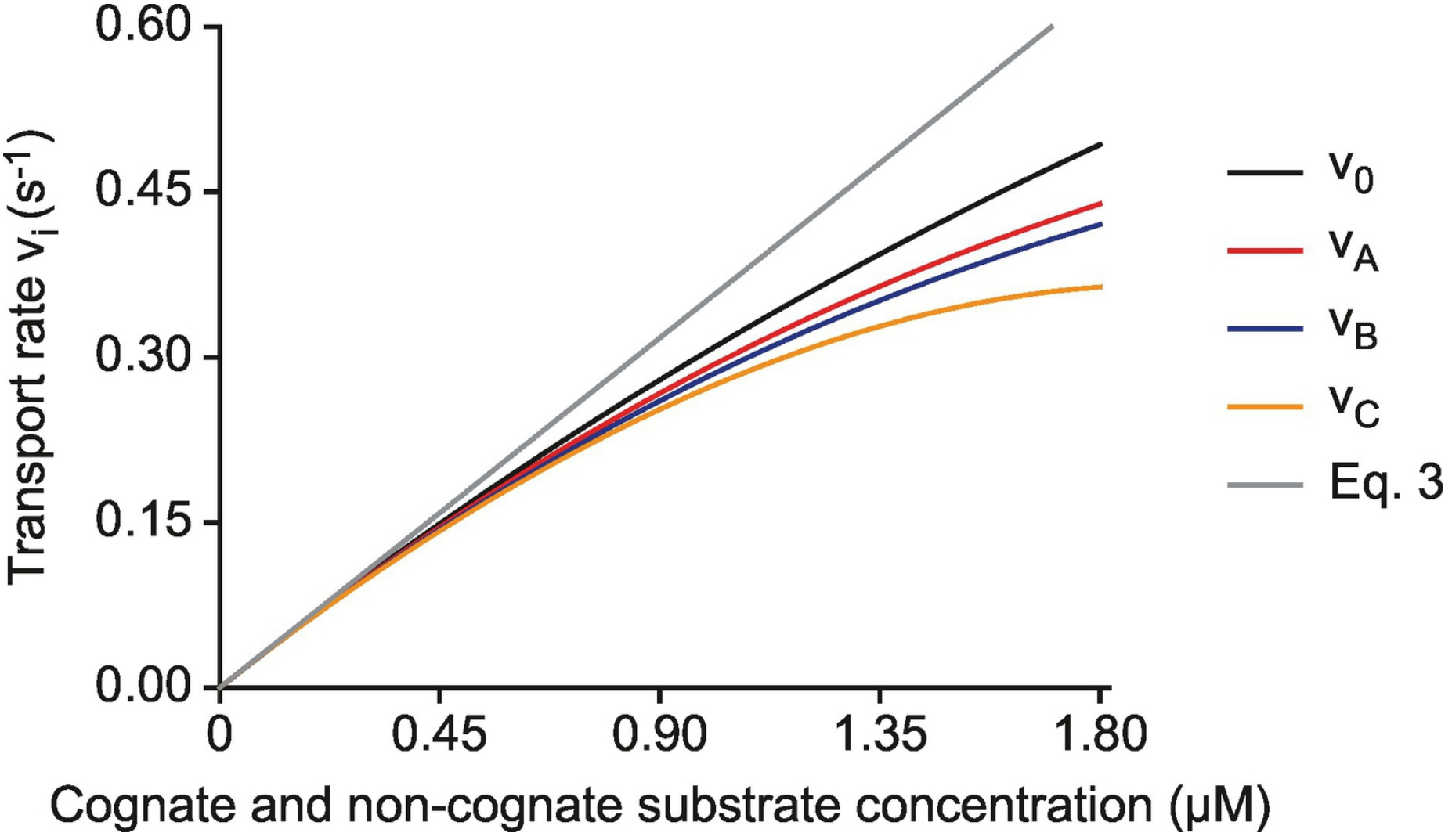
0.60
0.45
0.30
0.15
0.00
Transport rate v_i (s^{-1})
0
0.45
0.90
1.35
1.80
Cognate and non-cognate substrate concentration (μM)
v_0
v_A
v_B
v_C
Eq. 3

Figure 4

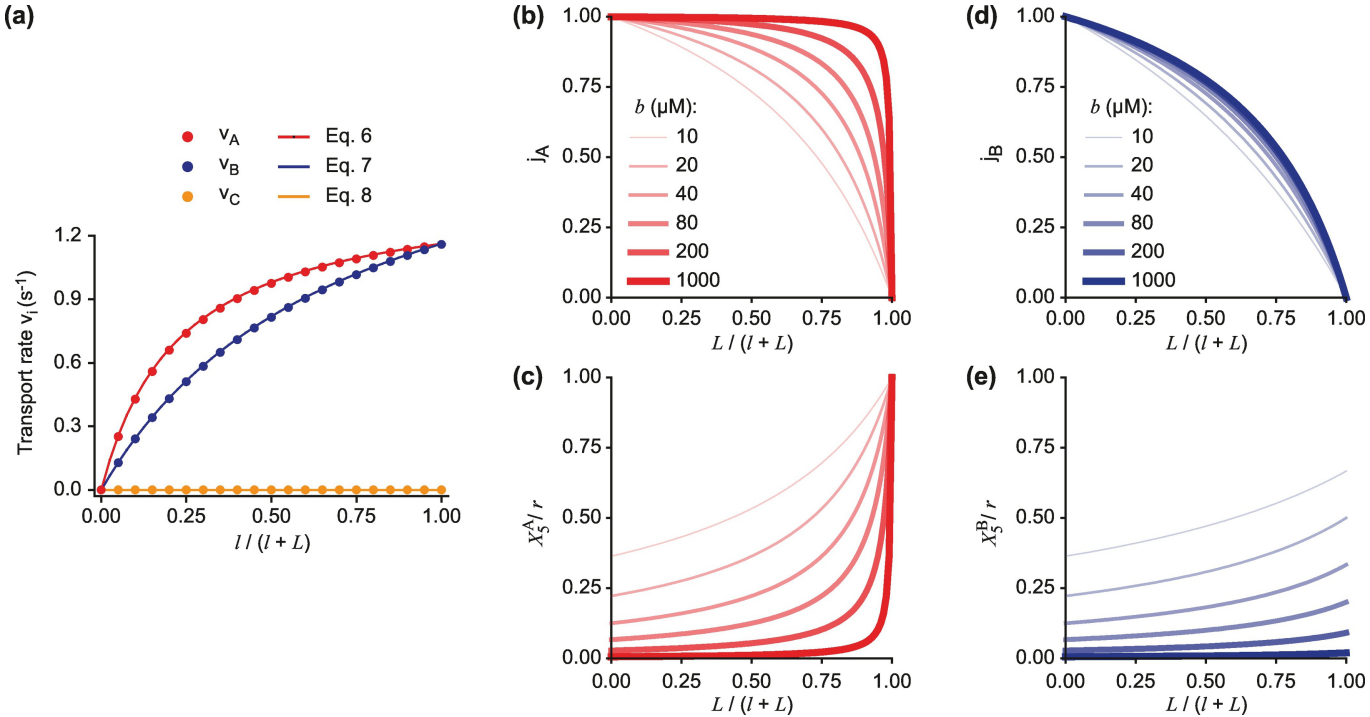
(a)
v_A
v_B
v_C
Eq. 6
Eq. 7
Eq. 8
Transport rate v_i (s^{-1})
1.2
0.9
0.6
0.3
0.0
0.00
0.25
0.50
0.75
1.00
l / (l + L)
(b)
j_A
b (μM):
10
20
40
80
200
1000
1.00
0.75
0.50
0.25
0.00
L / (l + L)
(d)
j_B
b (μM):
10
20
40
80
200
1000
(c)
x_5^A / r
(e)
x_5^B / r

Figure 5